ELSEVIER

Engineering Analysis with Boundary Elements 31 (2007) 209–215

ENGINEERING ANALYSIS with BOUNDARY ELEMENTS

www.elsevier.com/locate/enganabound

The singular function boundary integral method for biharmonic problems with crack singularities

Miltiades Elliotis, Georgios Georgiou*, Christos Xenophontos

Department of Mathematics and Statistics, University of Cyprus, P.O. Box 20537, 1678 Nicosia, Cyprus

Received 19 April 2006; accepted 14 September 2006
Available online 13 November 2006

Abstract

We use the singular function boundary integral method (SFBIM) to solve two model fracture problems on the plane. In the SFBIM, the solution is approximated by the leading terms of the local asymptotic solution expansion, which are also used to weight the governing biharmonic equation in the Galerkin sense. The discretized equations are reduced to boundary integrals by means of the divergence theorem and the Dirichlet boundary conditions are weakly enforced by means of Lagrange multipliers. The main advantage of the method is that the leading stress intensity factors (SIFs) are calculated directly together with the Lagrange multipliers, i.e. no post-processing of the numerical solution is necessary. The numerical results for the two model problems show the fast convergence of the method and compare well with those of the collocation Trefftz method.

Keywords: Biharmonic equation; Boundary singularity; Stress intensity factors; Singular function boundary integral method; Lagrange multipliers; Crack singularity

1. Introduction

In a recent work [1], we developed the Singular Function Boundary Integral Method (SFBIM) for plane elasticity problems. In this method, the solution is approximated by the leading terms of the local asymptotic solution expansion for the Airy stress function around the crack, which are referred to as the singular functions. The stress intensity factors (SIFs), also referred to as singular coefficients, are thus primary unknowns and are calculated directly. It should be noted that the idea for the above approximation has been known since the seventies; see, e.g., Ref. [2]. In the SFBIM, the singular functions are used to weight the governing biharmonic equation in the Galerkin sense, which allows the reduction of the discretized equations to boundary integrals by means of the divergence theorem. Lagrange multipliers are introduced in order to apply the Dirichlet boundary conditions. These are calculated together with the SIFs.

As already mentioned, one advantage of the SFBIM is the direct calculation of the SIFs. In other words, the method does not require post-processing of the numerical solution, which is not, in general, efficient and very accurate [3]. The method has been applied to Schiff's crack problem [1] exhibiting fast convergence with the number of singular functions and the number of Lagrange multipliers and yielding accurate estimates of the leading SIFs. The first SIF, in particular, was converged up to eight significant digits. The calculated SIFs agreed well with the collocation Trefftz method results of Li et al. [4]. In this method, the SIFs are also calculated directly, and as reported by Li et al. [4], the accuracy of the solutions is very high.

The objective of the present work is to test the performance of the SFBIM against the other two model problems (Model Problems I and II) studied by Li et al. [4], in which some numerical difficulties are posed by the presence of third-order partial derivatives in the boundary conditions. The paper is organized as follows: in Section 2, we present the two model problems and the corresponding asymptotic local solution expansion for the Airy stress function. In Section 3, the SFBIM is formulated for both

*Corresponding author. Tel.: +357 22892612; fax: +357 22892601.
E-mail address: georgios@ucy.ac.cy (G. Georgiou).

0955-7997/$ - see front matter © 2006 Elsevier Ltd. All rights reserved.
doi:10.1016/j.enganabound.2006.09.008

problems. In Section 4, numerical results showing the fast convergence of the method are presented and comparisons are made with the results of Li et al. [4]. Finally, the main conclusions are summarized in Section 5.

2. Governing equations and asymptotic solution

We consider here the Model Problems I and II studied by Li et al. [4]. These are shown in Figs. 1 and 2, respectively. In both problems, a rectangular thin elastic plate contains a single edge crack. Due to symmetry, only the upper half of the plate is considered, $\Omega = (-1,1) \times (0,1)$. Boundary parts S_A and S_B represent, respectively, the upper free surface of the crack and a horizontal plane section within the elastic interior of the material of the plate along the same direction of the crack plane. The crack is assumed to be very narrow in the limit of plane stress condition in the area of the crack, and hence boundary part S_A is taken as horizontal. In both problems, no shear stresses act on the upper and the left edges of the plate, S_D and S_E, respectively. What is different is the boundary condition along boundary part S_C. In Model Problem I, S_C represents a clamped edge, while in Model Problem II, S_C is a simply supported edge (i.e. without bending moments). In both problems, the Airy stress function $u(x,y)$ is governed by the biharmonic equation. The boundary conditions for the two problems are also depicted in Figs. 1 and 2.

The resulting boundary value problem in the case of Model Problem I is the following:

$$\nabla^4 u = 0 \quad \text{in } \Omega \tag{1}$$

with

$$\begin{aligned}
&u = 0, && \frac{\partial u}{\partial y} = 0 && \text{on } S_A,\\
&\frac{\partial u}{\partial y} = 0, && \frac{\partial^3 u}{\partial y^3} = 0 && \text{on } S_B,\\
&u = 1, && \frac{\partial u}{\partial x} = 0 && \text{on } S_C,\\
&\frac{\partial u}{\partial y} = 0, && \frac{\partial^3 u}{\partial y^3} = 0 && \text{on } S_D,\\
&\frac{\partial u}{\partial x} = 0, && \frac{\partial^3 u}{\partial x^3} = 0 && \text{on } S_E,
\end{aligned} \tag{2}$$

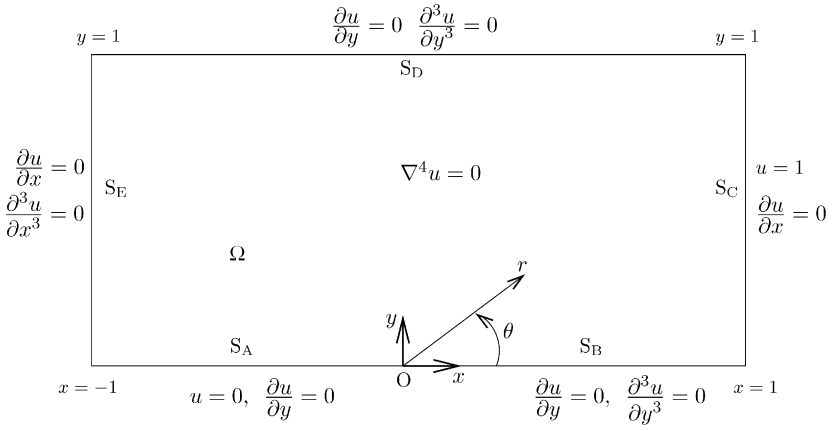

Fig. 1. Model Problem I.

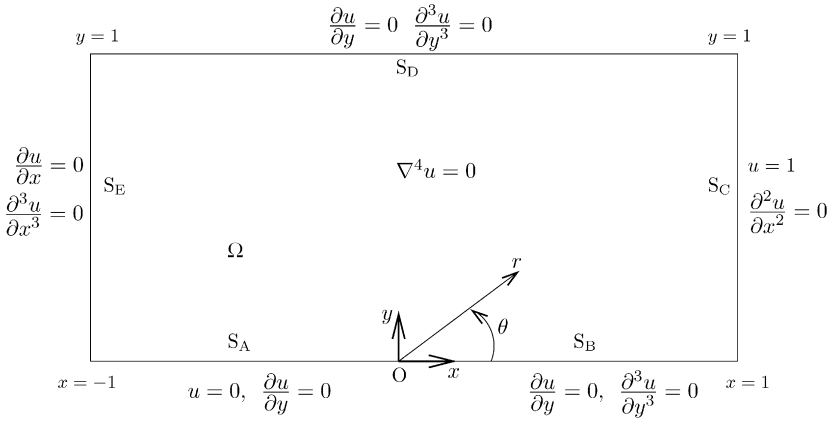

Fig. 2. Model Problem II.

where $S_A \cup S_B \cup S_C \cup A_D \cup S_E = \partial\Omega$. What is different in Model Problem II is the boundary condition along S_C

$$u = 1, \quad \frac{\partial^2 u}{\partial x^2} = 0 \quad \text{on } S_C. \tag{3}$$

Since the boundary conditions along boundary parts S_A and S_B are the same, the local asymptotic solution in the neighbourhood of the crack is the same in both model problems. This can be expressed in terms of an eigenfunction expansion of the form

$$u(r,\theta) = \sum_{j=1}^{\infty} a_j r^{\mu_j+1} f(\theta,\mu_j), \quad (r,\theta) \in \Omega, \tag{4}$$

where (r, θ) are the polar co-ordinates centred at the crack tip, O, α_j are the unknown SIFs, μ_j are the singularity powers arranged in ascending order, and the functions $f(\theta, \mu_j)$ represent the θ-dependence of the eigensolution. It turns out that the local solution (4) consists of two sets of particular solutions

$$W_1^j \equiv r^{\mu_j+1} f_1(\theta,\mu_j), \tag{5}$$

where

$$f_1(\theta,\mu_j) = \cos(\mu_j - 1)\theta - \frac{\mu_j - 1}{\mu_j + 1}\cos(\mu_j + 1)\theta,$$
$$\mu_j = j - \frac{1}{2}, \ j = 1,2,\ldots, \tag{6}$$

and

$$W_2^j \equiv r^{\mu_j+1} f_2(\theta,\mu_j), \tag{7}$$

where

$$f_2(\theta,\mu_j) = \cos(\mu_j - 1)\theta - \cos(\mu_j + 1)\theta,$$
$$\mu_j = j, \ j = 1,2,\ldots. \tag{8}$$

The functions W_1^j and W_2^j are referred to as the singular functions. Using the notation employed by Li et al. [4], the local asymptotic solution may be written as follows:

$$u = \sum_{j=1}^{\infty} d_j W_1^j + \sum_{j=1}^{\infty} c_j W_2^j, \tag{9}$$

where d_j and c_j are the SIFs corresponding to the two sets of singular functions. The first SIF, d_1 yields the opening mode SIF, $K = \sqrt{2\pi} d_1$ [5].

3. The singular function boundary integral method

In the SFBIM [1], the solution is approximated by the leading N_α terms of the local solution expansion (9)

$$\bar{u} = \sum_{j=1}^{N_\alpha} \bar{d}_j W_1^j + \sum_{j=1}^{N_\alpha} \bar{c}_j W_2^j, \tag{10}$$

where $\bar{u}$ is the approximation of the solution, and $\bar{c}_j$ and $\bar{d}_j$ are the approximations of the SIFs. The problem is discretized by applying Galerkin's principle, i.e. by weighting the governing biharmonic equation by the singular functions:

$$\int_\Omega \nabla^4 \bar{u} W_k^i \, \mathrm{d}V = 0, \quad i = 1,2,\ldots,N_\alpha, \ k = 1,2. \tag{11}$$

Noting that the singular functions W_k^j satisfy the biharmonic equation, the volume integrals are reduced to boundary ones by means of Green's theorem:

$$\int_{\partial\Omega} \left(\frac{\partial \bar{u}}{\partial n} \nabla^2 W_k^i - \bar{u} \frac{\partial (\nabla^2 W_k^i)}{\partial n} \right) \mathrm{d}S + \int_{\partial\Omega} \left(\frac{\partial (\nabla^2 \bar{u})}{\partial n} W_k^i - \nabla^2 \bar{u} \frac{\partial W_k^i}{\partial n} \right) \mathrm{d}S = 0, \quad i = 1,2,\ldots,N_a, \ k = 1,2. \tag{12}$$

The reduction of the problem dimension by one is clearly an important advantage of the method, as the computational cost is considerably reduced. Since the singular functions W_k^j also satisfy the boundary conditions along boundary parts S_A and S_B, the contributions of the latter to the boundary integrals of Eq. (12) are identically zero. Therefore, we can write

$$\int_{S_C \cup S_D \cup S_E} \left(\frac{\partial \bar{u}}{\partial n} \nabla^2 W_k^i - \bar{u} \frac{\partial (\nabla^2 W_k^i)}{\partial n} \right) \mathrm{d}S + \int_{S_C \cup S_D \cup S_E} \left(\frac{\partial (\nabla^2 \bar{u})}{\partial n} W_k^i - \nabla^2 \bar{u} \frac{\partial W_k^i}{\partial n} \right) \mathrm{d}S = 0, \quad i = 1,2,\ldots,N_a, \ k = 1,2. \tag{13}$$

There remains to enforce the Dirichlet boundary condition along S_C. This is applied in a weak sense by means of Lagrange multipliers, which may replace either the normal derivative $\partial\bar{u}/\partial n$ of the solution or $\partial\nabla^2\bar{u}/\partial n$ [1]. Since in Model Problem I, $\partial u/\partial x = 0$ along S_C, the Lagrange multipliers are chosen to replace $\partial(\nabla^2 u)/\partial x$. The Lagrange multiplier function, λ, is approximated locally by means of quadratic basis functions, M^j

$$\lambda = \left. \frac{\partial (\nabla^2 \bar{u})}{\partial x} \right|_{S_C} = \sum_{j=1}^{N_\lambda} \lambda^j M^j, \tag{14}$$

where N_λ is the number of the discrete Lagrange multipliers λ^j. The nodal values of λ are additional unknowns of the problem. The required N_λ additional equations are obtained by weighting, in the Galerkin sense, the Dirichlet condition along S_C by the quadratic basis functions M^i. Thus, the following linear system of $2N_\alpha + N_\lambda$ discretized equations is obtained

$$\int_{S_C} \left(\lambda W_k^i - \bar{u} \frac{\partial (\nabla^2 W_k^i)}{\partial x} - \nabla^2 \bar{u} \frac{\partial W_k^i}{\partial x} \right) \mathrm{d}y + \int_{S_D} \left(-\bar{u} \frac{\partial (\nabla^2 W_k^i)}{\partial y} + \frac{\partial^3 \bar{u}}{\partial y \partial x^2} W_k^i - \nabla^2 \bar{u} \frac{\partial W_k^i}{\partial y} \right) \mathrm{d}x + \int_{S_E} \left(\bar{u} \frac{\partial (\nabla^2 W_k^i)}{\partial x} - \frac{\partial^3 \bar{u}}{\partial x \partial y^2} W_k^i + \nabla^2 \bar{u} \frac{\partial W_k^i}{\partial x} \right) \mathrm{d}y = 0, \quad i = 1,\ldots,N_a, \ k = 1,2, \tag{15}$$

$$\int_{S_C} \bar{u} M^i \, dy = \int_{S_C} M^i \, dy, \quad i = 1, 2, \ldots, N_\lambda. \tag{16}$$

The integrands in the above equations are non-singular (all integrations are carried out far from the boundaries causing the singularity). Note that the stiffness matrix is symmetric and becomes singular when $N_\lambda > 2N_\alpha$, since the second set of equations does not contain the last N_λ unknowns (i.e. the discrete Lagrange multipliers).

In the case of Model Problem II, the Lagrange multiplier function has been chosen to replace the normal derivative of u, $\partial u/\partial x$, which in contrast to Model Problem I, is not zero

$$\lambda = \left.\frac{\partial \bar{u}}{\partial x}\right|_{S_C} = \sum_{j=1}^{N_\lambda} \lambda_C^j M^j. \tag{17}$$

What is different in the discretized equations (15) and (16) is just the boundary integral along S_C which reads

$$\int_{S_C} \left(\lambda \nabla^2 W_k^i - \bar{u} \frac{\partial (\nabla^2 W_k^i)}{\partial x} + \frac{\partial \nabla^2 \bar{u}}{\partial x} W_k^i - \frac{\partial^2 \bar{u}}{\partial y^2} \frac{\partial W_k^i}{\partial x} \right) dy.$$

Moreover, the resulting linear system is not symmetric. Let us note that we have also studied the possibility of λ replacing $\partial(\nabla^2 u)/\partial x$. It turns out that this alternative formulation gives essentially the same results, and it will not be discussed here.

As pointed out in Ref. [1], the SFBIM can be used only if the local asymptotic solution is known. Another limitation is the condition that the problem domain must be a subset of the domain of convergence of the asymptotic expansion. The same restrictions also hold for the collocation Trefftz method [4], with which comparisons are made in the next section.

4. Numerical results

In order to calculate the stiffness matrix and the force vector in Eqs. (15) and (16), boundary parts S_C, S_D and S_E, are partitioned uniformly into quadratic (i.e., 3-node) elements. Specifically, N_C elements are employed along each one of S_C and S_E, while $2N_C$ elements are used along S_D. Given that the partition of the boundary is uniform, the number of the quadratic elements used is determined from the number of Lagrange multipliers, i.e. $2N_C = (N_\lambda - 1)/2$. As in Refs. [1,6–8], the integrals in all formulations are calculated numerically by subdividing each element into 10 subintervals and using a 15-point Gauss–Legendre quadrature over each subinterval.

Systematic runs have been carried out in order to find the optimal values of the numbers of singular functions and Lagrange multipliers, N_α and N_λ. As already mentioned, $2N_\alpha$ must be greater than N_λ so that the stiffness matrix is non-singular. In fact, $2N_\alpha$ must be much greater than N_λ to avoid ill-conditioning of the stiffness matrix [1,6–8].

The effect of $2N_\alpha$ on the leading SIFs can be observed in Table 1, which shows the leading values of $\bar{c}_i$ and $\bar{d}_i$ for Model Problem I, obtained with $N_\lambda = 7$. We observe that fast convergence is achieved as $2N_\alpha$ is increased and accurate estimates of the leading SIFs are obtained. For $2N_\alpha = 50$ the results appear to be converged, while for higher values of N_α slow divergence is observed, due to the inaccuracies introduced by the high-order singular functions. For higher values of $2N_\alpha$ (e.g. $2N_\alpha = 56$) satisfactory

Table 1
Convergence of the leading SIFs with $2N_\alpha$; Model Problem I, $N_\lambda = 7$

$2N_\alpha$	c_1	c_2	c_3	c_4	c_5	c_{10}
30	1.579187	−1.01728	−0.39366	−0.12060	−0.01280	−0.00158
36	1.579371	−1.01748	−0.39417	−0.12014	−0.01265	−0.00112
40	1.579378	−1.01739	−0.39453	−0.11976	−0.01283	−0.00112
42	1.579372	−1.01742	−0.39424	−0.12007	−0.01269	−0.00111
44	1.579373	−1.01745	−0.39429	−0.12001	−0.01271	−0.00112
48	1.579373	−1.01746	−0.39427	−0.12003	−0.01270	−0.00112
50	1.579373	−1.01745	−0.39429	−0.12001	−0.01271	−0.00112
52	1.579373	−1.01746	−0.39425	−0.12005	−0.01269	−0.00112
54	1.579374	−1.01745	−0.39431	−0.11999	−0.01272	−0.00112
56	1.579373	−1.01746	−0.39426	−0.12004	−0.01270	−0.00112
58	1.579371	−1.01747	−0.39421	−0.12009	−0.01267	−0.00112
60	1.579377	−1.01741	−0.39445	−0.11985	−0.01279	−0.00112
$2N_\alpha$	c_1	c_2	c_3	c_4	c_5	c_{10}
30	0.07733	0.22801	0.14122	0.02777	−0.00589	0.00108
36	0.07692	0.22886	0.14089	0.02766	−0.00635	0.00080
40	0.07647	0.22942	0.14058	0.02770	−0.00628	0.00079
42	0.07683	0.22896	0.14082	0.02767	−0.00635	0.00076
44	0.07676	0.22905	0.14078	0.02768	−0.00633	0.00077
48	0.07679	0.22902	0.14079	0.02767	−0.00634	0.00077
50	0.07677	0.22905	0.14078	0.02767	−0.00633	0.00077
52	0.07682	0.22898	0.14081	0.02767	−0.00634	0.00077
54	0.07675	0.22907	0.14077	0.02768	−0.00633	0.00077
56	0.07680	0.22900	0.14080	0.02767	−0.00633	0.00077
58	0.07686	0.22892	0.14085	0.02767	−0.00635	0.00077
60	0.07657	0.22930	0.14064	0.02769	−0.00630	0.00078

Table 2
Convergence of the leading SIFs with N_λ; Model Problem I, $2N_\alpha = 50$

N_λ	d_1	d_2	d_3	d_4	d_5	d_{10}
3	1.579222	−1.01904	−0.38817	−0.12631	−0.00963	−0.00067
5	1.579304	−1.01820	−0.39139	−0.12300	−0.01127	−0.00097
7	1.579373	−1.01745	−0.39429	−0.12001	−0.01271	−0.00112
9	1.579373	−1.01745	−0.39428	−0.12002	−0.01271	−0.00112
11	1.579378	−1.01739	−0.39450	−0.11980	−0.01281	−0.00113
13	1.523493	−1.51039	1.54888	−2.11614	0.94649	0.05018
N_λ	c_1	c_2	c_3	c_4	c_5	c_{10}
3	0.08428	0.21940	0.14595	0.02707	−0.00772	0.00030
5	0.08032	0.22447	0.14323	0.02740	−0.00696	0.00062
7	0.07677	0.22905	0.14078	0.02767	−0.00633	0.00077
9	0.07678	0.22903	0.14079	0.02767	−0.00633	0.00077
11	0.07651	0.22937	0.14061	0.02769	−0.00629	0.00081
13	2.45544	−2.82869	1.77616	−0.01560	−0.41269	−0.05485

values of the SIFs are still obtained, but the quality of the global solution is not very good, as discussed below.

The convergence of the solution with the number of Lagrange multipliers is shown in Table 2, which contains the values of the leading SIFs for Model Problem I, calculated with $2N_\alpha = 50$ and various values of N_λ. Again, fast convergence is observed initially, up to $N_\lambda = 7$, but as N_λ increases the results diverge slowly, which is attributed to the fact that the stiffness matrix becomes ill-conditioned. Our computations showed that the optimum values of N_λ and $2N_\alpha$ are $N_\lambda = 7$ and $2N_\alpha = 50$. An indication of the quality of the solution is the smoothness of the calculated Lagrange multiplier function [1,6–8]. As shown in Fig. 3, for the optimum combination $N_\lambda = 7$ and $2N_\alpha = 50$, λ is smooth. For the slightly higher value of $N_\lambda = 9$, the estimated values of the SIFs are essentially the same, but

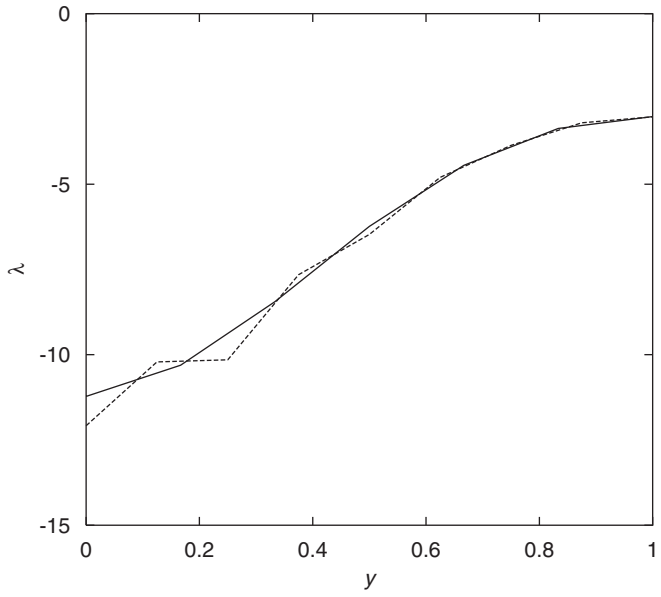

Fig. 3. Calculated Lagrange multipliers for Model Problem I with $2N_\alpha = 50$: $N_\lambda = 7$ (solid) and $N_\lambda = 9$ (dashed).

Table 3
Converged values of the SIFs for Model Problem I; $N_\lambda = 7$ and $2N_\alpha = 50$

i	d_i	c_i
1	1.579373	0.07677
2	−1.01745	0.22905
3	−0.39429	0.14078
4	−0.12001	0.02767
5	−0.01271	−0.00633
6	−0.00247	0.00612
7	−0.01542	0.01129
8	−0.01056	0.00511
9	−0.00343	0.00134
10	−0.00112	0.00077
11	−0.00091	0.00065
12	−0.00057	0.00031
13	−0.00022	0.00010
14	−0.00008	0.00006
15	−0.00006	0.00004

Table 4
Convergence of the leading SIFs with $2N_\alpha$; Model Problem II, $N_\lambda = 7$

$2N_\alpha$	d_1	d_2	d_3	d_4	d_5	d_{10}
30	0.843350	−0.08170	−0.07449	−0.04260	0.00032	0.00122
36	0.843270	−0.08140	−0.07487	−0.04181	0.00060	0.00015
40	0.843247	−0.08096	−0.07613	−0.04052	0.00115	0.00031
42	0.843263	−0.08103	−0.07601	−0.04065	−0.00108	0.00031
44	0.843264	−0.08103	−0.07602	−0.04064	−0.00108	0.00031
46	0.843264	−0.08103	−0.07601	−0.04065	−0.00108	0.00031
48	0.843262	−0.08102	−0.07602	−0.04063	−0.00109	0.00031
50	0.843238	−0.08101	−0.07593	−0.04073	−0.00105	0.00032
52	0.843366	−0.08124	−0.07598	−0.04069	−0.00100	0.00031
54	0.843324	−0.08114	−0.07603	−0.04063	−0.00105	0.00031
56	0.843333	−0.08116	−0.07602	−0.04065	−0.00104	0.00031
58	0.843346	−0.08110	−0.07628	−0.04038	−0.00116	0.00031
60	0.843460	−0.08142	−0.07598	−0.04071	−0.00093	0.00030
66	0.843231	−0.08132	−0.07490	−0.04181	−0.00052	0.00034

$2N_\alpha$	c_1	c_2	c_3	c_4	c_5	c_{10}
30	−0.13217	0.00292	0.04069	0.01445	−0.00986	−0.00069
36	−0.13298	0.00377	0.03992	0.01460	−0.00879	−0.00011
40	−0.13459	0.00573	0.03884	0.01472	−0.00871	−0.00012
42	−0.13441	0.00554	0.03895	0.01471	−0.00874	−0.00014
44	−0.13443	0.00556	0.03894	0.01471	−0.00874	−0.00014
46	−0.13442	0.00555	0.03895	0.01471	−0.00874	−0.00014
48	−0.13444	0.00557	0.03894	0.01471	−0.00874	−0.00014
50	−0.13435	0.00542	0.03901	0.01471	−0.00875	−0.00014
52	−0.13425	0.00550	0.03902	0.01467	−0.00879	−0.00013
54	−0.13437	0.00558	0.03896	0.01469	−0.00876	−0.00013
56	−0.13434	0.00556	0.03897	0.01469	−0.00876	−0.00014
58	−0.13466	0.00597	0.03875	0.01471	−0.00871	−0.00013
60	−0.13413	0.00549	0.03907	0.01464	−0.00882	−0.00014
66	−0.13304	0.00378	0.03991	0.01461	−0.00897	−0.00017

the Lagrange multiplier function exhibits oscillations. The converged values of the first 15 SIFs for Model Problem I are shown in Table 3.

The SFBIM appears to perform much better in the case of Model Problem II. The effect of $2N_\alpha$ on the leading SIFs can be observed in Table 4, which shows results obtained with $N_\lambda = 7$. Again, fast convergence is observed as $2N_\alpha$ is increased and accurate estimates of the leading SIFs are computed. The method appears to start diverging slowly for $2N_\alpha > 44$. The convergence of the SFBIM with the number of Lagrange multipliers is presented in Table 5, which shows the values of the leading SIFs calculated with $2N_\alpha = 44$ and various values of N_λ. The optimal values of N_λ and $2N_\alpha$ have been found to be $N_\lambda = 7$ and $2N_\alpha = 44$. As shown in Fig. 4, the corresponding Lagrange multiplier function is smooth, unlike its counterpart for $N_\lambda = 9$, which exhibits huge oscillations. The converged values of the first fifteen SIFs for Model Problem II are tabulated in Table 6.

Finally, as shown in Table 7, the converged values of coefficients d_1–d_{10} and c_1–c_{10} for both model problems compare well with the results of the collocation Trefftz method of Li et al. [4]. The latter researchers reported an accuracy of eight significant digits for d_1, but they do not

Table 5
Convergence of the leading SIFs with N_λ; Model Problem II, $2N_\alpha = 44$

$2N_\alpha$	d_1	d_2	d_3	d_4	d_5	d_{10}
3	0.845547	−0.08543	−0.07622	−0.04024	−0.00089	0.00041
5	0.843941	−0.08230	−0.07613	−0.04061	−0.00071	0.00024
7	0.843264	−0.08103	−0.07602	−0.04064	−0.00108	0.00031
9	0.843262	−0.08101	−0.07606	−0.04060	−0.00110	0.00031
11	0.844011	−0.08672	−0.06290	−0.05428	0.00540	0.00031
13	0.841944	−0.14174	−0.02388	−0.02233	0.04304	−0.00284
$2N_\alpha$	c_1	c_2	c_3	c_4	c_5	c_{10}
3	−0.13185	0.00607	0.03950	0.01341	−0.01050	−0.00058
5	−0.13371	0.00574	0.03915	0.01450	−0.00897	−0.00011
7	−0.13443	0.00556	0.03894	0.01471	−0.00874	−0.00014
9	−0.13448	0.00562	0.03891	0.01471	−0.00873	−0.00012
11	−0.11680	−0.14869	0.05044	0.01365	−0.01153	−0.00329
13	−0.03809	−0.02302	0.04203	−0.02431	−0.02142	−0.00192

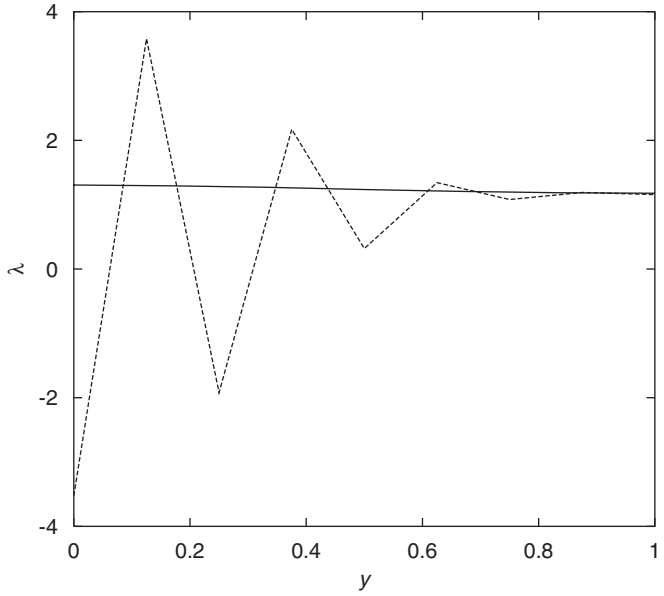

Fig. 4. Calculated Lagrange multipliers for Model Problem II with $2N_\alpha = 44$: $N_\lambda = 7$ (solid) and $N_\lambda = 9$ (dashed).

provide information about the convergence of the other SIFs. In Table 7 we tabulate their computed values with one additional digit than the converged values of the SFBIM. Agreement appears to be better in the case of Model Problem II. In fact, Li et al. [4] pointed out that their method is more accurate and stable in this problem.

5. Conclusions

The SFBIM has been used to solve two crack problems in the plane. The method converges rapidly with the number of singular functions and the number of Lagrange multipliers and gives directly accurate estimates of the leading SIFs. The results compare well with those of the Trefftz method used by Li et al. [4]. Despite their aforementioned limitations, both methods appear to be very attractive when the main goal is the computation of the SIFs.

The convergence of the SFBIM has been recently studied theoretically in the case of Laplace problems with boundary singularities [9,10]. In particular, it has been demonstrated that the method approximates the SIFs at an exponential rate [10]. The theoretical analysis of the convergence of the SFBIM in the case of the biharmonic equation with crack singularities is currently under investigation.

Table 6
Converged values of the SIFs for Model Problem II; $N_\lambda = 7$ and $2N_\alpha = 44$

i	d_i	c_i
1	0.843264	−0.13443
2	−0.08103	0.00556
3	−0.07602	0.03894
4	−0.04064	0.01471
5	−0.00108	−0.00874
6	0.00927	−0.00353
7	−0.00054	0.00153
8	−0.00160	0.00061
9	−0.00006	−0.00030
10	0.00031	−0.00014
11	−0.00002	0.00007
12	−0.00007	0.00003
13	−0.00000	−0.00002
14	0.00002	−0.00001
15	−0.00000	0.00000

Table 7
Comparison of the converged values of the SIFs with those obtained by Li et al. [4]

SIFs	Model Problem I		Model Problem II	
	Ref. [4]	SFBIM	Ref. [4]	SFBIM
d_1	1.579144	1.579373	0.8432657	0.843264
d_2	−1.018751	−1.01745	−0.081032	−0.08103
d_3	−0.388346	−0.39429	−0.076019	−0.07602
d_4	−0.126596	−0.12001	−0.040641	−0.04064
d_5	−0.009015	−0.01271	−0.001080	−0.00108
d_6	−0.004103	−0.00247	0.009265	0.00927
d_7	−0.015222	−0.01542	−0.000538	−0.00054
d_8	−0.010564	−0.01056	−0.001596	−0.00160
d_9	−0.003533	−0.00343	−0.000060	−0.00006
d_{10}	−0.001084	−0.00112	0.000313	0.00031
c_1	0.084557	0.07677	−0.134425	−0.13443
c_2	0.218683	0.22905	0.005557	0.00556
c_3	0.147059	0.14078	0.038943	0.03894
c_4	0.025896	0.02767	0.014708	0.01471
c_5	−0.006610	−0.00633	−0.008738	−0.00874
c_6	0.006926	0.00612	−0.003529	−0.00353
c_7	0.010900	0.01129	0.001525	0.00153
c_8	0.005336	0.00511	0.000619	0.00061
c_9	0.001285	0.00134	−0.000296	−0.00030
c_{10}	0.000799	0.00077	−0.000137	−0.00014

References

[1] Elliotis M, Georgiou G, Xenophontos C. The singular function boundary integral method for a two-dimensional fracture problem. Eng Anal Bound Elem 2006;30:100–6.
[2] Tong P, Pian THH, Lasry SJ. A hybrid-element approach to crack problems in plane elasticity. Int J Numer Meth Eng 1973;7: 297–308.
[3] Babuška I, Miller A. The post-processing approach in the finite element method — Part 2: the calculation of stress intensity factors. Int J Numer Meth Eng 1984;20:1111–29.
[4] Li ZC, Lu TT, Hu HY. The collocation Trefftz method for biharmonic equations with crack singularities. Eng Anal Bound Elem 2004;28:79–96.
[5] Irwin GR. Analysis of stresses and strains near the end of a crack traversing a plate. Trans ASME J Appl Mech 1957;24:361–4.
[6] Elliotis M, Georgiou G, Xenophontos C. The solution of a Laplacian problem over an L-shaped domain with a singular function boundary integral method. Commun Numer Meth Eng 2002;18:213–22.
[7] Elliotis M, Georgiou G, Xenophontos C. Solving Laplacian problems with boundary singularities: a comparison of a singular function boundary integral method with the p/hp version of the finite element method. Appl Math Comput 2005;169:485–99.
[8] Elliotis M, Georgiou G, Xenophontos C. Solution of the planar Newtonian stick-slip problem with the singular function boundary integral method. Int J Numer Meth Fluids 2005;48:1000–21.
[9] Li ZC, Chan YL, Georgiou GC, Xenophontos C. Special boundary approximation methods for Laplace equation problems with boundary singularities. Comp Math Appl 2006;51:115–42.
[10] Xenophontos C, Elliotis M, Georgiou G. A singular function boundary integral method for Laplacian problems with boundary singularities. SIAM J Sci Comput 2006;28:517–32.